Electronic Supplementary Material (ESI) for Chemical Communications.

Production of Janus/Hecate microfibers by microfluidic photopolymerization and evaluation of their potential in dyes removal

Wasif Razzaq,[a,b] Christophe Serra,[a,]* Delphine Chan-Seng[a]

[a] Université de Strasbourg, CNRS, Institut Charles Sadron UPR 22, F-67000 Strasbourg, France

[b] Department of Materials, National Textile University, Sheikhupura Road, Faisalabad, 37610, Pakistan

TABLE OF CONTENT

Materials

Tri(propylene glycol) diacrylate (Sartomer SR 306, TPGDA, Arkema), poly(ethylene glycol) diacrylate with M_n= 400 g/mol (PEGDA400, Polysciences), poly(ethylene glycol) diacrylate with M_n= 575 g/mol (PEGDA575, Sigma Aldrich), poly(ethylene glycol) diacrylate with M_n= 250 g/mol (PEGDA250, Sigma Aldrich), methyl bisacrylamide (99%, Sigma Aldrich), polyNOA89 (Norland), NOA74 (Norland), acrylamide (≥ 99%, Am, Sigma Aldrich), *N*-isoprylacrylamide (98%, NIPAm, TCI), *n*-butyl acrylate (99%, *n*-BA, TCI), *tert*-butyl acrylate (98%, *tert*-BA, TCI), acrylic acid (≥99.0, AA, Sigma Aldrich), 2-(dimethyl amino) ethyl acrylate) (98%, DMAEA,TCI), Irgacure 369 (Ciba), Irgacure 2959 (Sigma Aldrich), ethanol (99.9%, Carlo Erba), methylene blue (extra, MB, Merck), alizarin red S sodium salt (AR, Alfa Aesar), crystal violet (Merck), rhodamine 6G (for microscopy, Merck), poly(ethylene glycol) with a molecular weight of 300 g/mol (PEG300, Sigma Aldrich), hydrochloric acid (≥37%, HCl, Sigma Aldrich), potassium hydroxide (≥ 85%, KOH, Carl Roth) were used as received. For the preparation of the amphoteric Janus fiber, reversed-osmosed water was used.

Side-by-side capillary-based microfluidic device

The side-by-side capillary-based microfluidic system consisted of PEEK T-junctions, fused silica glass capillaries, sleeves, and PTFE tubings. The microfluidics arrangement used for producing Janus fibers is illustrated in Fig. 1a and below. The two T-junctions (PEEK) were connected to each other using a sleeve. The first capillary (internal diameter (I.D) = 50 µm, outer diameter (O.D) = 150 µm, red) started from the left of T-junction and passing through the two sleeves and exit from the right T-junction and is used to deliver the core phase 1 (Φ_{core1}). The second capillary (I.D = 50 µm, O.D = 150 µm) started from the exit of first T-junction and passing through the sleeve 2 and exit at the end of second T-junction and is used to deliver the core phase 2 (Φ_{core2}). The tips of two capillaries at the exit of second T-junctions were glued together with epoxy adhesive (superglue) in a way that there is almost no gap in between them. The exit tips of the two capillaries were placed in the centerline of an outlet PTFE tubing (I.D = 1.56 mm). Downstream to the capillaries tip, a 20 cm long outlet tubing section was exposed to UV irradiations (Lighting cure LC 8, Hamamatsu) operating at λ = 365 nm and full intensity (100%). Under these conditions, the parallel streams of two monomers were polymerized in *ca*. 0.34 (min) to 0.87 (max) minutes. The contact point between the sheath and core fluids (capillary tip) was observed using an optical microscope (SMZ 171, Motic) equipped with a camera (MotiCam 5, Motic). For the production of Hecate fibers, the capillaries used had the following characteristics: I.D = 100 µm and O.D = 150 µm, while the inner diameter of outlet tubing was 2.1 mm.

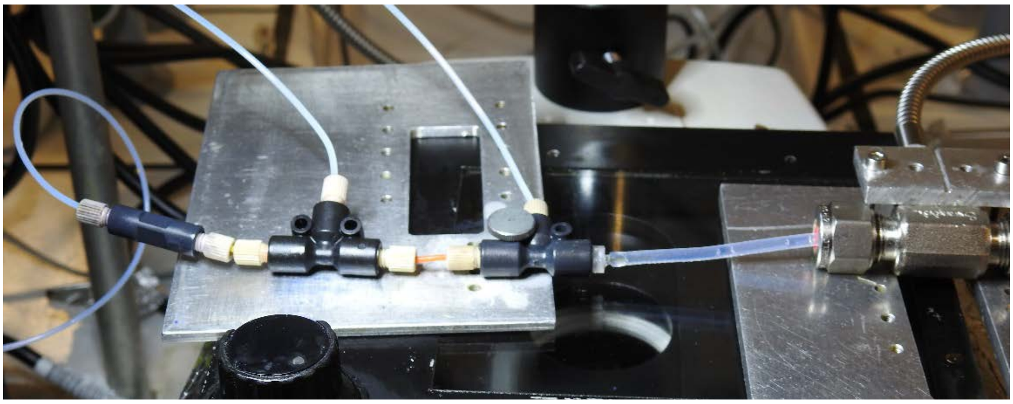

Characterization techniques

The overall diameter and the width of each parts of Janus and Hecate of the microfibers were measured using a numerical microscope (Keyence, VHX-J100T) with variable resolution ranging from 100 to 1000x . Scanning electron microscopy (SEM) images were obtained on a Hitachi SU 8010 Ultra High-Resolution FE-SEM microscope at 1.0 kV. The fibers placed on the sample holder were held with carbon tape (Agar Scientific).

The elastic modulus was determined by dynamic mechanical analysis (DMA) on a Mettler Toledo DMA 1 by clamping an individual fiber between the jaws of DMA and using an oscillating frequency of 1 Hz under control amplitude at 20 °C.

UV-vis spectroscopy was carried out using a Perkin Elmer Lambda 25 spectrophotometer into quartz cuvettes at room temperature.

Adsorption studies

Determination of the removal efficiency. All experiments were conducted in batch experiments at 20 °C using 20 mg of amphoteric AA/DMAEA Janus fibers immersed in 15 mL of 20 mg/L of MB or AR in reverse-osmosed water. The pH of the dye solutions was adjusted to 7 and 6 respectively. 3 mL aliquots of the solutions were withdrawn at predetermined times. The change in dye concentration was monitored by UV-vis spectroscopy at 664 and 406 nm for MB and AR respectively. The experiment was continued until no change in concentration was observed (equilibrium). The amount of dye adsorbed was calculated using the calibration curves which were preestablished for each dye.

The removal efficiency (RE%) of the dyes by adsorption on the fibers was calculated as follows:

$$RE\% = \frac{c_i - c_t}{c_i} \times 100$$

Determination of the adsorption capacity. The experiments were conducted in batch experiment under the following conditions: adsorbent dosage = 20 mg, volume of dye solution = 50 mL, temperature = 293.15 K, time = 8 h for MB and 3 h for AR, pH = 7 for MB and 6 for AR. The adsorption capacity (in mg of dye per gram of fibers) at the equilibrium (q_e) and at time t (q_t) was calculated using the following equations:

$$q_e = \frac{(c_i - c_e) \times V}{m} \quad \text{and} \quad q_t = \frac{(c_i - c_t) \times V}{m}$$

where c_i, c_t, and c_e are the concentrations in dye at time zero, time t, and when the equilibrium is reached respectively, q_e and q_t the adsorption capacities of dyes at equilibrium time and time t respectively.

Adsorption kinetics. To analyze the mechanism of dye adsorption onto the amphoteric Janus fiber absorbent, the data obtained from the effect of contact time were fitted to the linear forms of the pseudo-first and pseudo-second order kinetic models listed below.

$$\log(q_e - q_t) = \log(q_e) - \frac{k_1 t}{2.303} \qquad \textit{for the pseudo-first order model}$$

$$\frac{t}{q_t} = \frac{1}{k_2 q_e^2} + \frac{t}{q_e} \qquad \textit{for the pseudo-second order model}$$

where q_t is the adsorption capacities at time t and q_e the predicted adsorption capacity at equilibrium time. k_1 and k_2 are the pseudo-first and pseudo-second order rate constants. The values of k_1, k_2, and predicted q_e can be calculated from the slope and intercept of plots $\log(q_e - q_t)$ *vs.* t for pseudo-first order model and t/q_t *vs.* t for pseudo-second order model.

Adsorption isotherms. Adsorption isotherms usually elaborate the interactive behavior between the adsorbent and dye molecules and also provide the information about the adsorption capacity (mg of dye/g of adsorbent) of the dye in solution. Langmuir and Freundlich models are the most suitable models for understanding the interaction between the dye molecules and adsorbent. The Langmuir model relates to the homogenous and monolayer adsorption of dye on adsorbent, while the Freundlich model is based on the assumption of heterogeneous surface and multilayer adsorption. Adsorption capacities were investigated using different initial concentrations in dye and the data was fitted into the Langmuir and Freundlich isotherm models. Their linear forms are expressed below.

Langmuir isotherm model $\frac{C_e}{q_e} = \frac{1}{K_L q_m} + \frac{C_e}{q_m}$

where c_e is the equilibrium concentration in dye, q_e the equilibrium adsorption capacity of the fibers, q_m and K_L are Langmuir constants in which q_m represents the maximum adsorption capacity while b relates to the affinity and free energy towards the adsorption. A dimensionless constant separation parameter (R_L) is one of the essential information describing the type of adsorption isotherm and reveals the favorability of the adsorption in the Langmuir model. R_L can be obtained by the following equation: $R_L = \frac{1}{(1+C_o K_L)}$, where c_o is initial concentration in dye. The adsorption isotherm may be favorable (if $R_L > 1$), linear (if $R_L = 1$), favorable (if $0 < R_L < 1$), or irreversible (if $R_L = 0$).

Freundlich isotherm model $\ln q_e = \ln K_f + \frac{1}{n} \ln c_e$

where K_f and n are Freundlich constants related to capacity of the adsorbent and intensity of adsorption.

Supplementary Figures

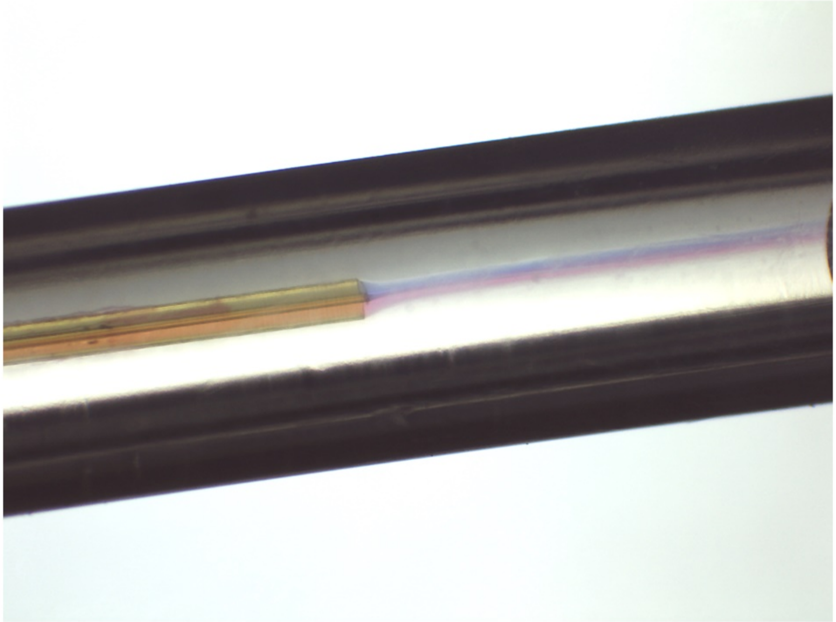

Fig. S1. Optical image revealing the co-flow of two core phases at the capillary tips using crystal violet in Φ_{core1} and rhodamine 6G in Φ_{core2}.

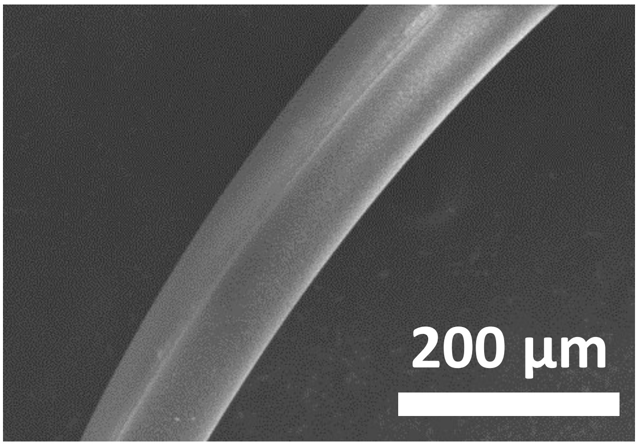

Fig. S2. SEM image of the Janus fibers prepared in Fig. 1 using TPGDA and NOA89 after 8 months.

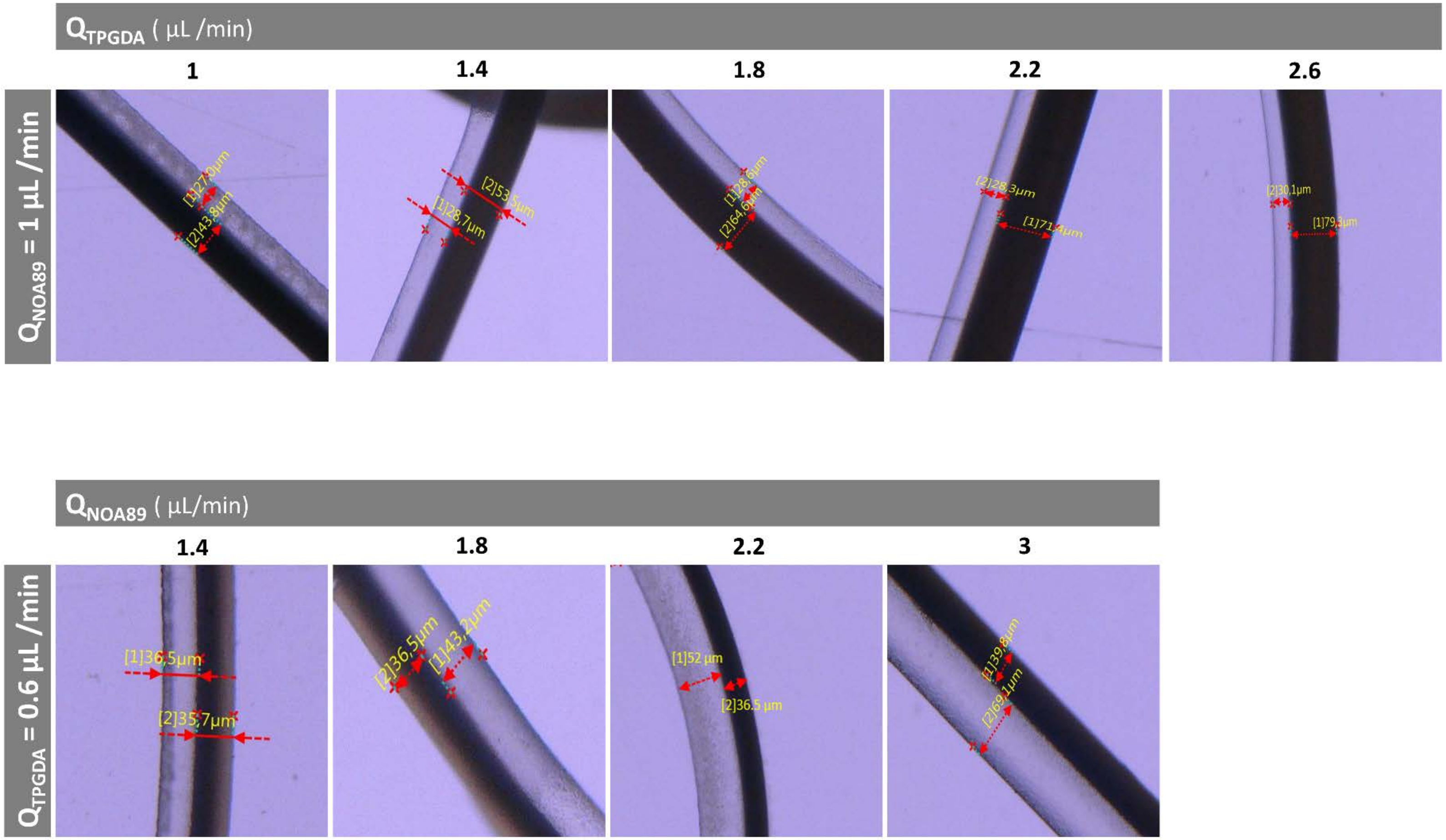

Fig. S3. Numerical images of TPGDA/NOA89 Janus fibers showing the evolution in width of each part of the fiber when increasing the flow rate of one of the core phases while keeping the other one constant.

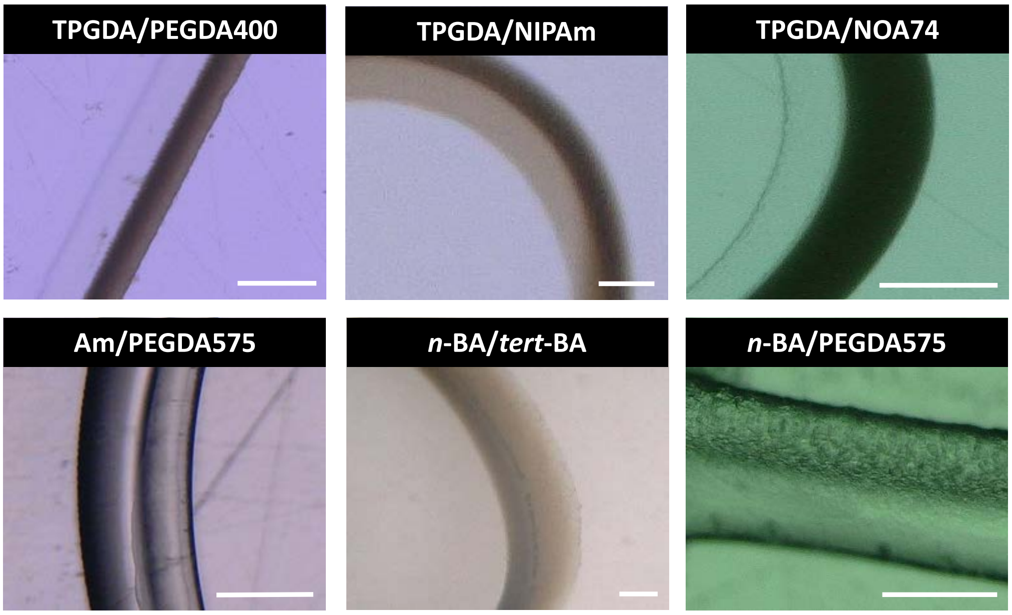

Fig. S4. Numerical microcopy images of Janus fibers produced using different monomer combinations (scale bar = 100 µm). The differences in background colors is due to the contrast corrections done to better observe both parts of the Janus microfibers.

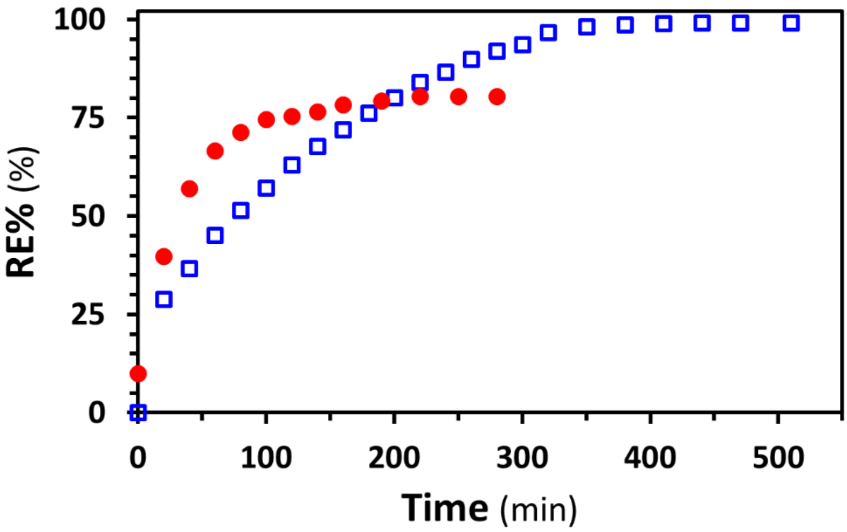

Fig. S5. Effect of the contact time on the removal efficiency of MB (□) and AR (●) dyes for amphoteric AA/DMAEA Janus fibers.

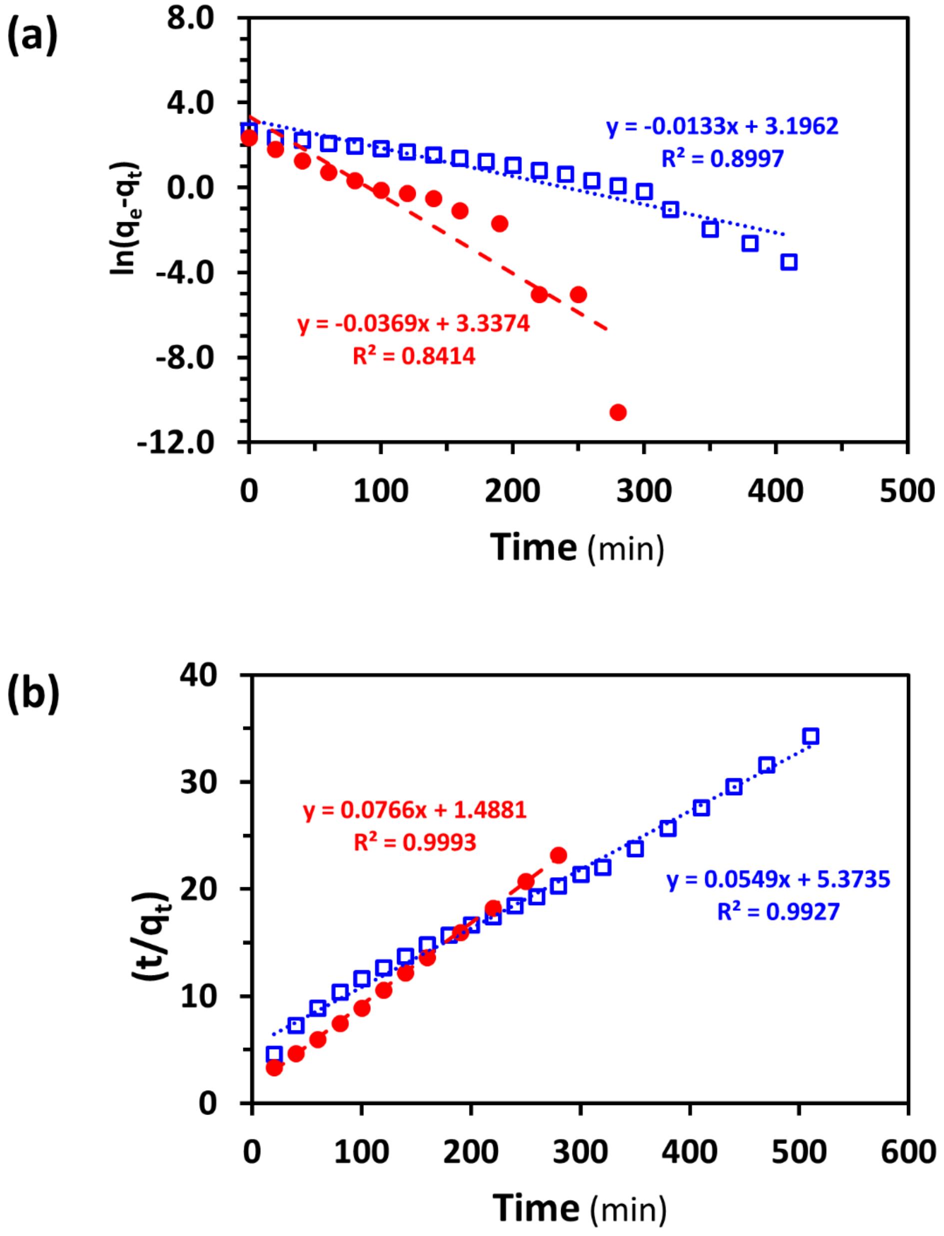

Fig. S6. Adsorption kinetic of MB (□) and AR (●) onto amphoteric Janus microfibers using (a) pseudo-first and (b) pseudo-second order kinetic models.

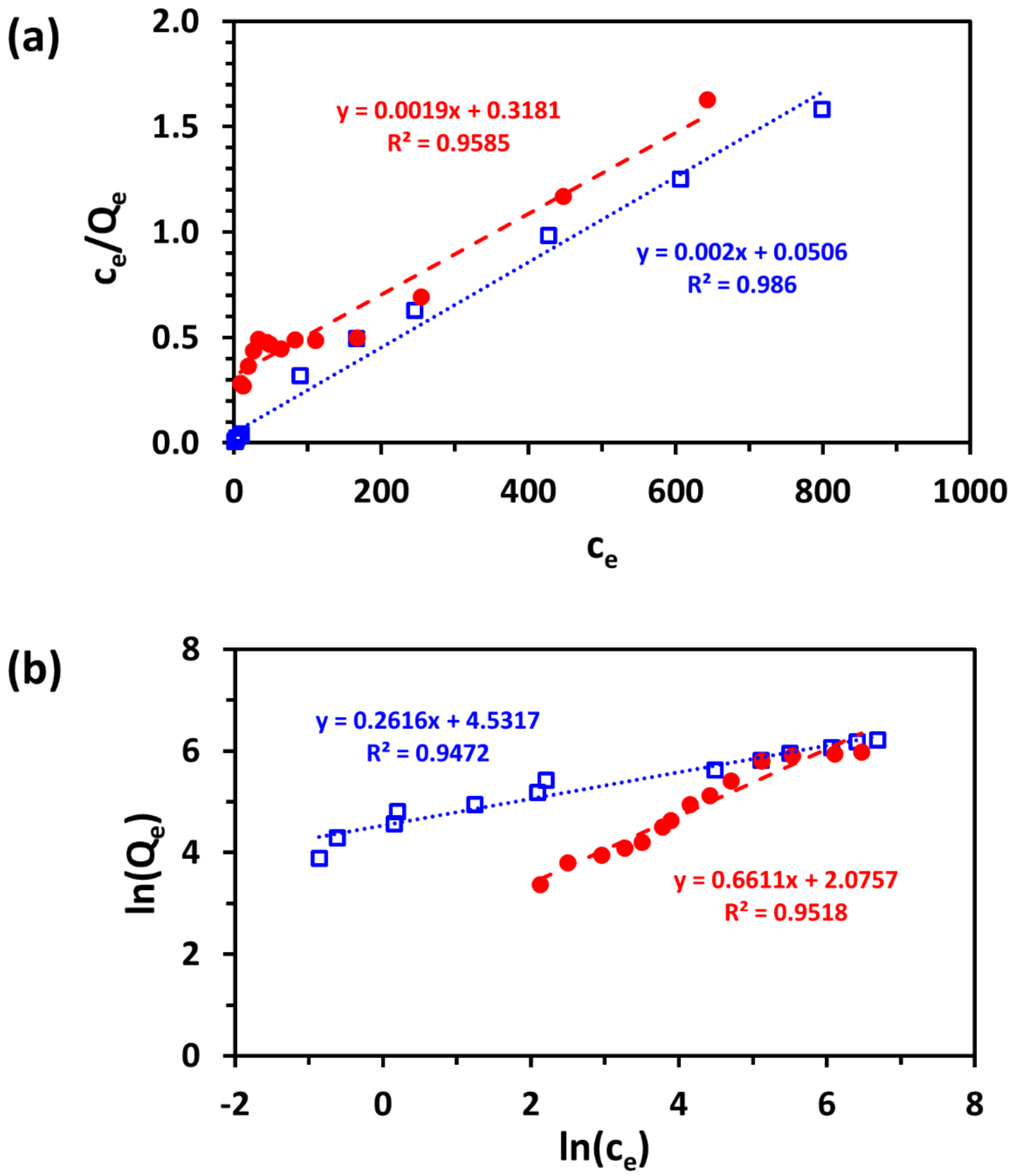

Fig. S7. Adsorption isotherm for MB (□) and AR (●) onto amphoteric AA/DMAEA Janus fibers (a) Langmuir and (b) Freundlich models.

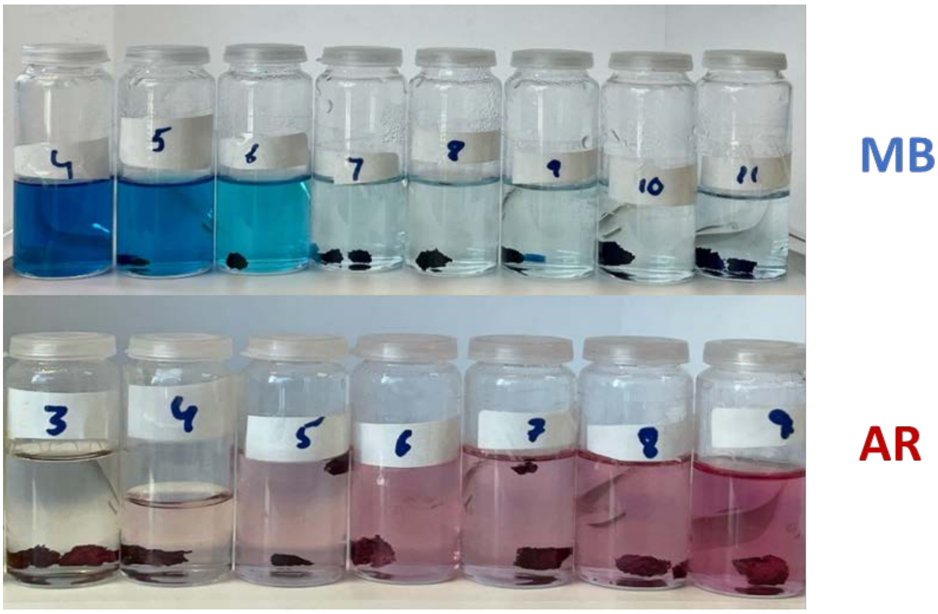

Fig. S8. Dye solutions at different pH after immersion of amphoteric AA/DMAEA Janus fibers after reaching the equilibrium time (the number on the vial corresponds to the pH of the solution).

Fig. S9. Image showing the precipitate observed when both dyes (MB and AR) were used in the same solution.

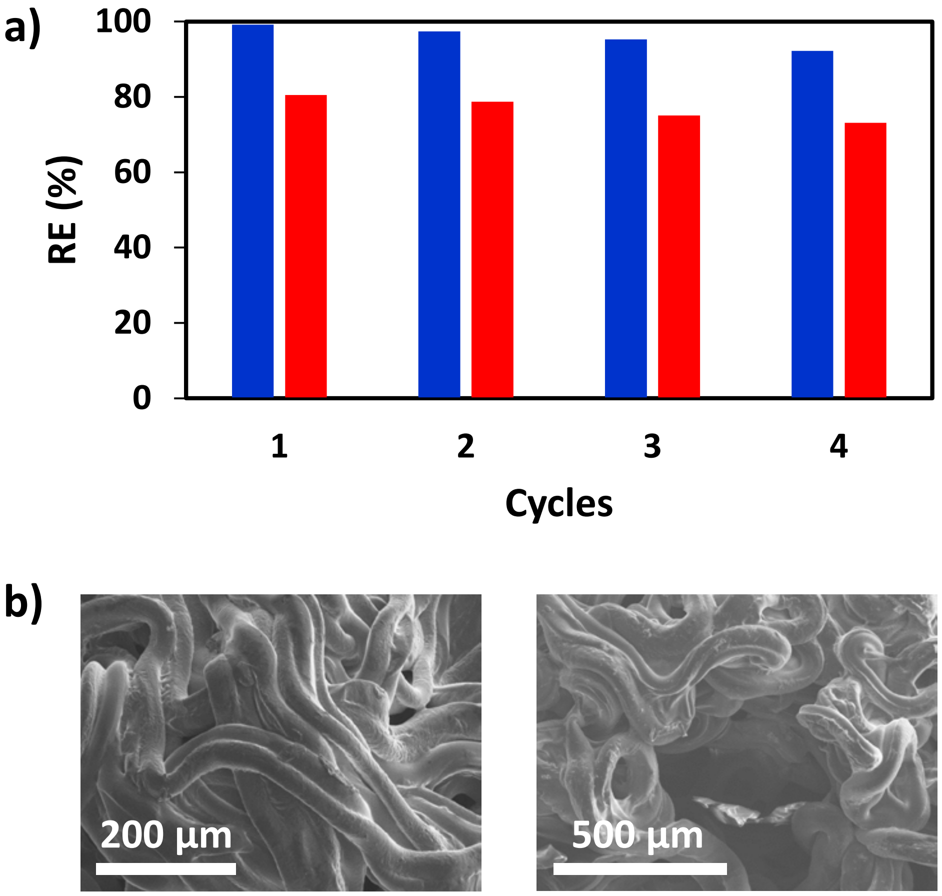

Fig. S10. Adsorption/desorption cycles of MB (blue column) and AR (red column) onto amphoteric Janus fibers: a) adsorption capacity after different numbers of cycles and b) SEM images of the fibers before and after three cycles.

Supplementary Tables

Table S1. Summary of the kinetic and isotherm parameters for the adsorption of MB or AR on amphoteric AA/DMAEA Janus fibers.

Model	**Kinetic parameter**	**MB**	**AR**
Pseudo-first order	k_1 (10^{-4})(min^{-1})	0.28	1.32
	R^2	0.899	0.841
	q_{exp} (mg/g)	14.87	12.07
	q_{cal} (mg/g)	24.43	28.14
Pseudo-second order	K_2 (10^{-3}) (g/mg*min)	0.56	3.94
	R^2	0.9927	0.9993
	q_{exp} (mg/g)	14.87	12.07
	q_{cal} (mg/g)	18.21	13.05
Langmuir isotherm	q_{max} (mg/g)	500	526.31
	K_L (L/mg)	0.039	0.006
	R^2	0.986	0.956
Freundlich isotherm	n (L/mg)	3.822	1.512
	K_F (mg/g)	92.92	7.97
	R^2	0.947	0.952

Table S2. Separation constant R_L from the Langmuir model according to the initial dye concentration in solution for MB and AR.

C_o (mg/L)	**R_L**	
	MB	**AR**
100	0.202	0.626
200	0.112	0.455
400	0.0595	0.295
600	0.040	0.218
800	0.030	0.173
1000	0.024	0.143

Table S3. Comparison of the adsorption capacity of PAA/PDMAE Janus fibers with fibers reported in the literature for the removal of MB and/or AR.[a]

Fibers	**Adsorption capacity** (mg/g)		**Reference**
	MB	**AR**	
Molecularly imprinted sericin/poly(vinyl alcohol) fibers	223	-	1
Polydopamine-modified fibers	15	-	2
Etherified cellulose	410	-	3
Functionalized carbon nanofibers	172	-	4
Hydrolyzed PIM-1 ultrafine fibers	157	-	5
β-Cyclodextrin-based fibers	826	-	6
Crosslinked polycyclodextrin/polybenzoxazine microfibers	46		7
phenolic resin/cotton fiber composites	-	133	8
PVC/CNT nanocomposite fibers	-	15	9
Multiwalled carbon nanotubes	-	161	10
PAA/PDMAE amphoteric Janus fibers	504	394	this work

[a] Studies in red involve microfibers (1-10 μm), the others nanofibers

References

1. R. Zhao, X. Li, B. Sun, Y. Li, Y. Li and C. Wang, *Chem. Res. Chin. Univ.*, 2017, **33**, 986-994.
2. C. Wang, J. Yin, R. Wang, T. Jiao, H. Huang, J. Zhou, L. Zhang and Q. Peng, *Nanomaterials*, 2019, **9**, 116.
3. X. Shao, J. Wang, Z. Liu, N. Hu, M. Liu, C. Duan, R. Zhang and C. Quan, *Cellulose*, 2021, **28**, 9355-9367.
4. B. M. Thamer, H. El-Hamshary, S. S. Al-Deyab and M. H. El-Newehy, *Arabian J. Chem.*, 2019, **12**, 747-759.
5. B. Satilmis, P. M. Budd and T. Uyar, *React. Funct. Polym.*, 2017, **121**, 67-75.
6. R. Zhao, Y. Wang, X. Li, B. Sun and C. Wang, *ACS Appl. Mater. Interfaces*, 2015, **7**, 26649-26657.
7. Y. E. Dogan, B. Satilmis and T. Uyar, *Eur. Polym. J.*, 2019, **119**, 311-321.
8. B. Wanassi, I. B. Hariz, C. M. Ghimbeu, C. Vaulot and M. Jeguirim, *Energies*, 2017, **10**, 1321.
9. M. Hasan, R. Kumar, M. A. Barakat and M. Lee, *RSC Adv.*, 2015, **5**, 14393-14399.
10. M. Ghaedi, A. Hassanzadeh and S. N. Kokhdan, *J. Chem. Eng. Data*, 2011, **56**, 2511-2520.